Effect of a baffle divertor structure on neutral hydrogen and helium transport in the Large Helical Device

M. Shoji[a*], S. Masuzaki[a], M. Kobayashi[a], H. Funaba[a], T. Morisaki[a], H. Yamada[a] and the LHD Experiment Group[a]

[a]*National Institute for Fusion Science, 322-6 Oroshi-cho, Toki 509-5292,Gifu, Japan*

Abstract

Control of the peripheral plasma density is one of urgent tasks for improving the plasma performance in the Large Helical Device. Test modules with a baffle divertor structure have been installed in the inboard side of the torus for controlling the neutral density in the plasma periphery. Neutral hydrogen and helium transport in an original open divertor and the baffle divertor configurations have been monitored with filtered CCD cameras to observe the intensity profile of visible emission by neutral hydrogen (H_α) and helium (HeI). A detailed analysis using a three-dimensional neutral particle transport simulation code reasonably explains the dependence of the observed intensity profiles on the divertor and the magnetic configurations. It also predicts that the baffle divertor significantly reduces the emission of neutral hydrogen in the plasma periphery in the inboard side, and the compression of neutral helium density by the baffle divertor is comparable to that of hydrogen.

PACS: 52.20.Hv, 52.25.Ya, 52.55.Hc, 52.70.Kz

PSI-20 Keywords: Divertor neutrals, Divertor geometry, EIRENE, Helium, LHD

**Corresponding Author Address: National Institute for Fusion Science, 322-6 Oroshi-cho, Toki 509-5292, Japan*

**Corresponding Author e-mail:* shoji@LHD.nifs.ac.jp

Presenting Author: Mamoru Shoji

Presenting Author e-mail: shoji@LHD.nifs.ac.jp

1. Introduction

Recent plasma discharge experiments in the Large Helical Device (LHD) have demonstrated that control of the peripheral plasma density is essential for achieving super dense core (SDC) and sustaining ICRF heated long pulse discharges [1, 2]. It has also been recognized that peripheral plasma density control is critical to sustain high ion temperature with an internal transport barrier (ITB) with an impurity hole [3].

For active control of the plasma density, full torus installation of a closed divertor was proposed. Fully three-dimensional neutral particle transport simulation for the closed divertor configuration predicts that enhancement of neutral particle density behind a dome structure by more than one-order of magnitude compared to that in the original open divertor configuration. In order to check the performance of the closed divertor, two test modules with a baffle divertor structure were installed in the inboard side of the torus in 2010. Comparison between the measurements of the neutral particle pressure in the baffle divertor and those in the open divertor clearly showed the enhancement of the neutral pressure as predicted by the neutral particle transport simulation [4].

In addition to checking the enhancement of the neutral particle density, investigation of the effect of the test module on neutral particle transport in the divertor region is an important topic for improving the closed divertor. The analysis of transport of helium atoms is also an issue to optimize the design of the closed divertor in future helical fusion reactors for effective helium ash removal. The transport of neutral helium atoms is quite different from that of hydrogen atoms/molecules because of the higher ionization energy and no molecular dissociation processes, etc. Thus, analysis using sophisticated neutral particle transport simulation is required.

The experimental campaign in 2011 was a good opportunity to check the performance of the test module on neutral particle transport in the divertor region. This is because we could simultaneously measure the neutral transport with fast ionization gauges

and filtered CCD cameras in the both divertor regions under same main plasma conditions. In this paper, the intensity profiles of the visible emission by neutral hydrogen and helium measured with the filtered CCD cameras are shown in the both divertor configurations for the two different magnetic configurations. The observations are analyzed by a fully three-dimensional neutral particle transport simulation code to show the effect of the test modules on the control of neutral transport and on the helium pumping.

2. Experimental setup

The LHD is the largest super-conducting heliotron-type device, with a set of l=2, m=10 helical coils and three pairs of poloidal coils. The edge magnetic field line structure outside the last closed flux surface (LCFS) consists of an ergodic layer, residual islands, and an edge-surface layer [5]. Four bundled magnetic field lines (divertor legs) are deviated from the ergodic layer at two X-points and directly connect to divertor plates (carbon) which are helically installed along strike points to protect the vacuum vessel (stainless steel) from the plasma heat flux.

Figure 1 illustrates a half torus cross-section of the vacuum vessel on the equatorial plane for showing the position of the test modules and experimental setup of plasma diagnostic systems for measuring neutral particle pressure and the intensity profiles of visible emission in the divertor regions. The test module consists of three components: baffle divertor plates, target plates and a roof-shaped dome structure, which effectively confine neutral particles released from the divertor plates behind the dome (see Figure 1 in reference 6). The test module (baffle divertor) is installed only in the inboard side of the torus because calculations of magnetic field line tracing show that about 80% of the strike points locate in the inboard side for an inward magnetic axis shift configuration in which the best energy confinement time has been achieved in the LHD [7]. A cryo-sorption panel cooled by helium gas will be installed behind the dome in near future for pumping neutral particles in the

divertor region.

Neutral particle transport in the baffle divertor and the open divertor regions has been routinely monitored with filtered CCD cameras (Toshiba IK-UM44H and IK-CU44) and fast ionization gauges [8]. Two appended illustrations in the left side in Figure 1 are graphical images of the divertor geometries viewed from the two camera positions. Figure 2 is a perspective view of the experimental setup and the viewing area of the cameras in the both divertor configurations with showing the lines of sight of the cameras (gray lines).

3. Measurements of the intensity profiles of visible emission

The upper images in Figure 3 and 4 are the measured intensity profiles of two visible emission of neutral hydrogen (H_α: λ=656.3nm) and helium (HeI: λ=587.6nm) observed with the filtered cameras for monitoring the baffle and the open divertor in typical NBI heated plasmas in the case where the radial position of the magnetic axis (R_{ax}) is 3.60m and 3.75m, respectively. The magnetic field line configurations in the plasma periphery and on the inner divertor legs are changed with the position of the magnetic axis (see Figure 1 in reference 2). In the two magnetic configurations, thick and thin divertor legs (~10 cm and ~2cm in width) are formed in the inboard sides, respectively. The main plasma parameters in the two magnetic configurations are almost the same (an electron density at the LCFS: n_e^{LCFS}~5×10^{19}m^{-3}, an electron temperature in the plasma center: T_{e0}~2keV). The intensity profiles of the visible emission were measured in hydrogen fuelled plasmas after several tenth discharges with additional helium gas injection. The spectroscopic measurements of the ratio of the hydrogen and residual helium ions in the plasma periphery showed that the ratio of hydrogen on the total ions is more than 90% [9].

For R_{ax}=3.60m (Figure 3), the intensity profiles in the both divertor configurations are similar, showing a dark stripe along the area between the two lines of the inner divertor

plates (private region). In the case of R_{ax}=3.75m (Figure 4), the intensity profiles in the private region has no clear structures (almost uniform) in the both divertor configurations. The figures also indicate no observable difference of the intensity profile of the emission between neutral hydrogen (H_α) and helium (HeI) under the different divertor and magnetic configurations.

4. Neutral particle transport analysis in the open and the baffle divertor configurations

Understanding reasons for the change of the observed intensity profile by the divertor and magnetic configurations is an important issue for improving the performance of the closed divertor. Therefore, the effect of the baffle divertor on neutral particle (hydrogen and helium) transport in the two magnetic configurations is investigated using a fully three-dimensional neutral particle transport simulation code (EIRENE) [10, 11]. In this simulation, density profiles of neutral particles are calculated by tracking many test particles representing neutral hydrogen atoms and molecules, helium atoms in three-dimensional grid models. Atomic/molecular processes of hydrogen and helium included in the code are charge exchange, ion/electron impact ionization and electron impact dissociation (hydrogen molecules). The shape of LHD plasmas, the vacuum vessel and the structure of the baffle and open divertor configurations for one toroidal pitch angle ($0°<\phi<36°$) are included in the models as precise as possible. Two toroidal edge surfaces in the models are treated as periodic surfaces for simulating the full torus geometry. The structure of the test module is constructed as a component made of some triangular ‘additional surfaces’ from which neutral particles are released into the model. It is assumed that the current of released neutral particles linearly depends on the plasma current onto the surfaces of the divertor plates, and the kinetic energy of neutral hydrogen molecules and helium atoms desorbed from the divertor plates corresponds to that of room temperature (300K).

A simple neutral particle balance analysis in the LHD showed the presence of strong

hydrogen pumping on the divertor plates and the vacuum vessel [12]. Microscopic studies of deposition layers on the surface of the divertor plates proved that a large amount of hydrogen is retained in co-deposition layers of mixed material composed of carbon and metallic impurities [13]. In the neutral particle transport simulation, a particle reflection coefficient of hydrogen/helium on the divertor plates (R_N) is set to 0.65/1.0 in order to include the pumping effect of hydrogen, which reproduces typical measurements of the neutral particle pressure in the inboard side for the open divertor configuration [4]. It is assumed that carbon atoms fully cover the surface of the vacuum vessel by physical and chemical sputtering on the divertor plates, which is experimentally supported by a microscopic analysis of the deposition layers on fixed-type material probes installed on the vacuum vessel [14].

The plasma parameter profiles inside the ergodic layer are calculations by a three-dimensional plasma fluid code (EMC3-EIRENE) in the open divertor configuration [15]. Cross-field particle transport coefficient (D) in the code is set to be 0.4m^2/s for R_{ax}=3.60m, and 0.5m^2/s for R_{ax}=3.75m, respectively. It is assumed that electron and ion thermal conductivity follow the following formula: $\chi_e=\chi_i=3\times D$. These parameters are fixed so as to make the calculated electron density and temperature profiles consistent with measured radial profiles in the ergodic layer [16]. The plasma parameters in fine grids for the plasma fluid code are mapped to coarse grids specialized for the neutral particle transport simulation by a volume averaging process. Since the plasma fluid code cannot calculate the plasma parameter profiles on the divertor legs because of deformation of grids by the large rotational transform of the magnetic field lines in the plasma periphery, the calculation domain is extended so as to include the divertor legs by introducing a one-dimensional plasma fluid analysis along magnetic field lines. It provides the three-dimensional profile of the plasma parameters on the divertor legs using the plasma parameters at the upstream of the divertor legs calculated by the plasma fluid code and the effect of neutral particles calculated by the EIRENE [11].

The spatial profile of H_α emission is calculated by a module in the EIRENE. The

spatial profile of HeI emission is obtained by introducing a module for analyzing the observations of HeI intensity profiles in direct helium gas injection experiments, which was used for a neutral particle transport simulation code (DEGAS 2) [17, 18]. The contribution of the continuum light from helium ions on HeI emission is ignored because the ratio of residual helium ions is low (less than 10%) in the LHD plasmas for this analysis.

5. Calculations of emission profiles in the open and the baffle divertor configurations

Figure 5 (a) gives the poloidal cross sections of the calculated emission profile of H_α ($\varepsilon_{H\alpha}$) and HeI (ε_{HeI}) in the both divertor configurations for R_{ax}=3.60m at a toroidal angle where the plasma is horizontally elongated. The emission on the ergodic layer in the inboard side of the torus for the baffle divertor is reduced by a factor of about 2 compared to that for the open divertor. It means that the baffle divertor effectively functions for controlling the neutral density in the plasma periphery in this magnetic configuration. The emission profile of the neutral helium is localized in the outer boundary of the ergodic layer because of the short mean free path of helium which is estimated to be about 3cm in typical peripheral plasmas in the LHD [9]. It is much smaller than the plasma minor radius (~0.8m) and the width of the ergodic layer (~0.2m). Figure 5 (b) is poloidal cross sections of the emission profile for R_{ax}=3.75m, showing that the baffle divertor is also effective for reduction of the neutral density in the plasma periphery. But, the effect of the baffle divertor in this magnetic configuration is moderate compared to that for R_{ax}=3.60m.

In the case of R_{ax}=3.60m, the simulation indicates that the baffle divertor can enhance neutral helium density behind the dome by about one-order of magnitude compared to that in the open divertor, which shows that the effect of the baffle divertor on helium pumping is equivalent to that of hydrogen one. For R_{ax}=3.75m, the enhancement of the neutral helium density in the baffle divertor is about 7 which is also equivalent to that of hydrogen. It indicates that the baffle divertor shows the best performance of neutral particle (hydrogen and

helium) pumping for R_{ax}=3.60m. Fortunately, it is favorable for LHD plasma operation because the best energy confinement time with maximum stored energy has been achieved in this magnetic configuration.

Line integration of the visible emission along the lines of sight of the cameras provides the intensity profile of H_α and HeI emission. Lower images in Figure 3 and 4 are the calculated intensity profiles in the two magnetic configurations (R_{ax}=3.60m and 3.75m, respectively) by integrating the emission along totally 14,000 lines of sight, which shows that the calculated intensity profiles in the both divertor configurations reproduce the measured profiles. The dark stripe in the private region in the both divertor configurations for R_{ax}=3.60m is explained by the presence of the thick divertor legs in the inboard side. Most of neutral particles are ionized on the inner divertor legs or on the ergodic layer near the divertor plates. The simulation explains that the reason why the intensity profile in the private region for R_{ax}=3.75m has no clear structures (almost uniform) is due to distributed emission profiles on the inner divertor legs and on the ergodic layer in the inboard side. This is because neutral particles released from the divertor plates can penetrate the thin inner divertor legs and widely ionized on the ergodic layer in this magnetic configuration.

6. Summary

Fully three-dimensional analysis using a neutral particle transport simulation code is a powerful method to understand the observed intensity profiles of the emission of neutral particles (hydrogen and helium) in the different divertor and magnetic configurations. The calculated intensity profiles reproduce the observations, which proves that the dark stripe of the intensity profile in the private region for R_{ax}=3.60m is explained by ionization of neutral particles on the thick inner divertor legs. The almost uniform intensity profile in the private region for R_{ax}=3.75m is due to penetration of neutral particles through the thin divertor legs in the inboard side. The simulation predicts that the emission on the ergodic layer in the inboard

side for the baffle divertor configuration is reduced by a factor of about 2 compared to that for the open divertor configuration, which means that the baffle divertor effectively works for controlling the peripheral plasma density. It also indicates that enhancement of helium density by the baffle divertor is comparable to that of hydrogen, showing the effective helium pumping in the baffle divertor configuration. This is the first demonstration of the possibility of helium ash removal in helical/stellarator-type devices. The neutral particle transport analysis for R_{ax}=3.75m shows that the effect of the baffle divertor becomes moderate compared to that for R_{ax}=3.60m.

Acknowledgements

This work is supported by the LHD numerical analysis system and is performed under the auspices of the NIFS Collaboration Research program (NIFS08KNXN131).

References

[1] N. Ohyabu et al., Phys. Rev. Lett. 97 (2006) 055002.

[2] M. Shoji et al., Fusion Sci. Technol 56 (2009) 1001.

[3] K. Ida et al., Phys. Plasmas 16 (2009) 056111.

[4] S. Masuzaki et al., Plasma and Fusion Res. 6 (2011) 1202007-1.

[5] S. Masuzaki et al., Nucl. Fusion 42 (2002) 750.

[6] M. Shoji et al., J. Nucl. Mater. 415 (2011) S557.

[7] H. Yamada et al., Nucl. Fusion 45 (2005) 1684.

[8] G. Haas, et al., J. Nucl. Mater. 121 (1984) 151.

[9] M. Goto et al., Phys. Plasmas 10 (2003) 1402.

[10] D. Reiter et al., Fusion Sci. Technol. 47 (2005) 172.

[11] M. Shoji et al., J. Nucl. Mater. 390-391 (2009) 490.

[12] M. Kobayashi et al., J. Nucl. Mater. 350 (2006) 40.

[13] M. Tokitani et al., J. Nucl. Mater. 367-370 (2007) 1487.

[14] T. Hino et al., Nucl. Fusion 44 (2004) 496.

[15] Y. Feng et al., Plasma Phys. Control. Fusion 44 (2002) 611.

[16] M. Kobayashi et al., Fusion Sci. and Technol. 58 (2010) 220.

[17] D.P. Stotler et al., J. Nucl. Mater. 363-365 (2007) 686.

[18] M. Goto et al., J. Quant. Spectros. Radiat. Transfer 76 (2003) 331.

Figure captions

Fig. 1. A half torus cross-section of the vacuum vessel on the equatorial plane for showing the position of the test modules and the experimental setup of diagnostics for monitoring the neutral particle transport in the baffle and the open divertor regions.

Fig. 2. Three-dimensional models for the neutral particle transport simulation in the baffle and the open divertor configurations with showing the position of filtered CCD cameras and its viewing areas.

Fig. 3. Observations (upper images) and calculations (lower images) of the intensity profiles of visible emission of neutral hydrogen (H_α) and helium (HeI) in the baffle and the open divertor configurations for R_{ax}=3.60m.

Fig. 4. Observations (upper images) and calculations (lower images) of the intensity profiles of visible emission of neutral hydrogen (H_α) and helium (HeI) in the baffle and the open divertor configurations for R_{ax}=3.75m.

Fig. 5. The poloidal cross-sections of the calculated emission profiles of neutral hydrogen (H_α) and helium (HeI) in the baffle and the open divertor cases for the two magnetic configurations (R_{ax}=3.60m (a) and 3.75m (b)).

Figure

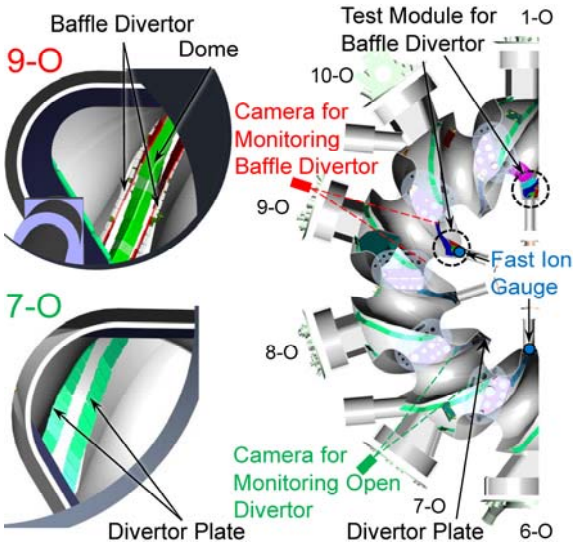

Figure 1

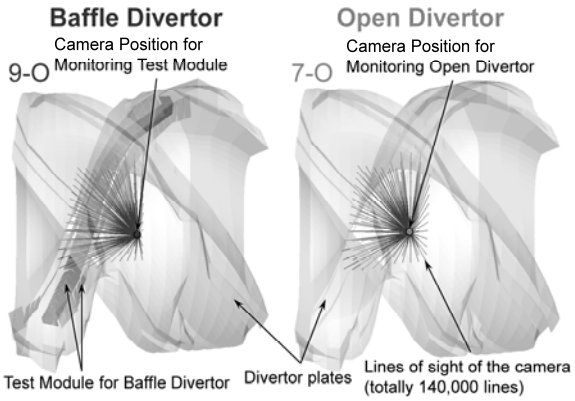
Baffle Divertor
Camera Position for
Monitoring Test Module
9-O
Open Divertor
Camera Position for
Monitoring Open Divertor
7-O
Test Module for Baffle Divertor
Divertor plates
Lines of sight of the camera
(totally 140,000 lines)

Figure 2

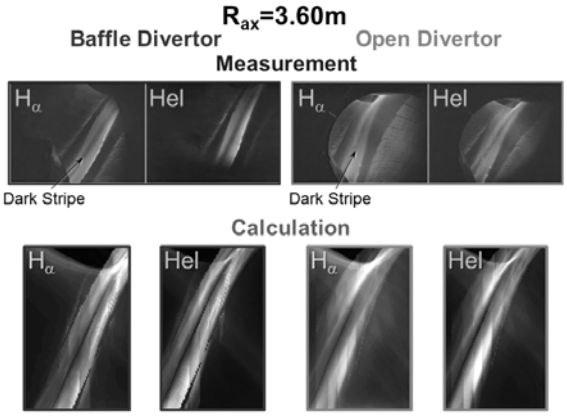
R_{ax}=3.60m
Baffle Divertor
Open Divertor
Measurement
H_α
HeI
H_α
HeI
Dark Stripe
Dark Stripe
Calculation
H_α
HeI
H_α
HeI

Figure 3

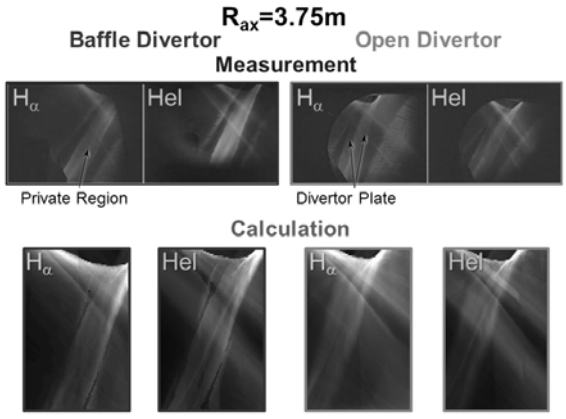
R_{ax}=3.75m
Baffle Divertor
Open Divertor
Measurement
H_α
HeI
H_α
HeI
Private Region
Divertor Plate
Calculation
H_α
HeI
H_α
HeI

Figure 4

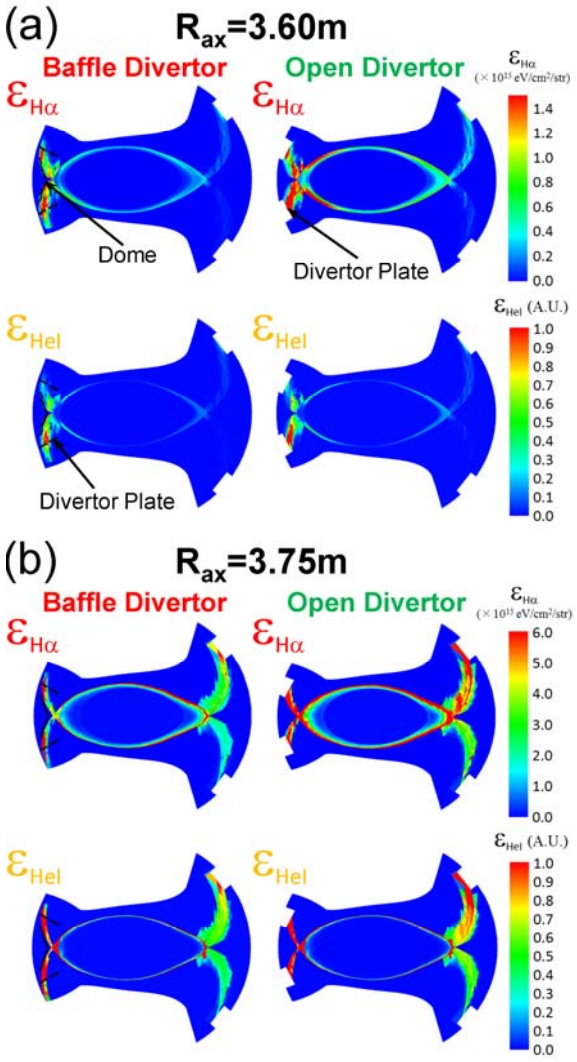
(a)
R_{ax}=3.60m
Baffle Divertor
Open Divertor
$\varepsilon_{H\alpha}$
$\varepsilon_{H\alpha}$
$\varepsilon_{H\alpha}$ ($\times 10^{15}$ eV/cm^2/str)
1.4
1.2
1.0
0.8
0.6
0.4
0.2
0.0
Dome
Divertor Plate
ε_{Hel}
ε_{Hel}
ε_{Hel} (A.U.)
1.0
0.9
0.8
0.7
0.6
0.5
0.4
0.3
0.2
0.1
0.0
Divertor Plate
(b)
R_{ax}=3.75m
Baffle Divertor
Open Divertor
$\varepsilon_{H\alpha}$
$\varepsilon_{H\alpha}$
$\varepsilon_{H\alpha}$ ($\times 10^{15}$ eV/cm^2/str)
6.0
5.0
4.0
3.0
2.0
1.0
0.0
ε_{Hel}
ε_{Hel}
ε_{Hel} (A.U.)
1.0
0.9
0.8
0.7
0.6
0.5
0.4
0.3
0.2
0.1
0.0

Figure 5